Physics of the Earth and Planetary Interiors 178 (2010) 92–99

Contents lists available at ScienceDirect

Physics of the Earth and Planetary Interiors

journal homepage: www.elsevier.com/locate/pepi

Subduction of the Western Pacific Plate underneath Northeast China: Implications of numerical studies

Guizhi Zhu[a,*], Yaolin Shi[b], Paul Tackley[a]

[a] Department of Earth Sciences, Swiss Federal Institute of Technology (ETH-Zurich), CH-8092 Zurich, Switzerland
[b] Laboratory of Computational Geodynamics, Graduate University of Chinese Academy of Sciences, 100049 Beijing, China

ARTICLE INFO

Article history:
Received 9 January 2009
Received in revised form 25 October 2009
Accepted 26 October 2009

Edited by K. Zhang.

Keywords:
Deep subduction
Northeast China
Western Pacific plate
Trench retreat

ABSTRACT

The geodynamic process of the deep subduction of the western Pacific Plate underneath Northeast China is critical for understanding the extensional events and volcanism in Northeast China. Understanding of this process depends on: (1) the initial time of the subduction, (2) the trench retreat velocity during the subduction process, (3) the contribution of Indian-Eurasian collision and Pacific-Eurasian subduction to extensional events in the northeast of China. However, information on these three issues is very limited. We use several regional models to gain insight into these three issues. Each of the models includes temperature-dependent viscosity structures, and distinct velocity patterns at the surface. Our results show that the subduction of the Pacific Plate under the Eurasian plate started most probably around 70 Ma. To be consistent with the tomography under Northeast China, trench retreat must be included in the models, with a rate less than 45 km/Ma that has been estimated in the past. We suggest that the extension events in the northeast China are attributed to Indian-Eurasian collision and Pacific-Eurasian subduction according to the velocity evolution in our models.

1. Introduction

Northeast (NE) China is located in a complicated region with westward subduction of the Pacific plate (Liu et al., 2001; Northrup et al., 1995; Sun and He, 2004; Zang and Ning, 1996; Huang and Zhao, 2006) and distant effects of India-Eurasia collision (Liu et al., 2004; Molnar and Tapponnier, 1975; Molnar and Tapponnier, 1977). The causes of some geophysical and geological phenomena in NE China are still under debate. For instance, some researchers support the plume hypothesis (e.g., Bi, 1997; Duncan and Richards, 1991) for volcanoes in NE China because volcanoes and extensional events there are far from the oceanic trench, but seismic tomography shows that the Cenozoic volcanoes, which are not plume-related, are located above the subducting slab at about 600 km depth (Huang and Zhao, 2006; Zhao, 2004; Zhao et al., 2007). However, seismic observations give us some clues. Seismicity in NE China indeed has some relation to the subduction of the Japan Sea plate (Sun and He, 2004; Zang and Ning, 1996), we can also get the seismicity catalogue (during 1964–2005) from the official website: http://www.iris.edu, as shown in Fig. 1. Geochemical volcanic data have shown that Cenozoic episodic volcanism and continental rifting in NE China have some link to Japan Sea development (Liu et al., 2001; Shi and Zhang, 2004). Thus, the understanding of the western subduction of the Pacific Plate underneath NE China becomes important with the constraints of geological history in Cenozoic times and current tomography results, as illustrated in Fig. 2.

From current tomography (Huang and Zhao, 2006; Zhao et al., 2007), the subduction process involves two parts. One is flat subduction, the other is stagnant slabs above the 660-km discontinuity, and the part that lies flat is about 1000 km long. As for flat subduction, it is commonly related to trench retreat according to numerical simulations (Zhong and Gurnis, 1997; Becker et al., 1999) and laboratory experiments (Guillou-Frottier et al., 1995; Funiciello et al., 2003a,b). For this region, there are some uncertainties, including the initial subduction time of the Pacific Plate underneath NE China, the trench retreat velocity and the viscosity structure. Shi and Zhang (2004) estimated that the initial subduction time of western subduction of the Pacific Plate underneath NE China is approximately 45 Ma and the lying flat process of the subducting slab started at around 28 Ma. Liu and Wang (1982) estimated that the migration rate of Cenozoic volcanism is averagely 45 mm/year, that is, 45 km/Ma.

In this paper, we use a regional incompressible mantle convection model for the region shown in Fig. 1 in spherical projection to simulate the process of the western subduction of the Pacific Plate underneath NE China with the constraints of the tomography results (Huang and Zhao, 2006; Zhao et al., 2007), migration rate

* Corresponding author at: Department of Earth Sciences, Swiss Federal Institute of Technology (ETH-Zurich), CH-8092 Zurich, Switzerland. Tel.: +41 44 633 2907; fax: +41 44 6321080.
E-mail address: guizhi.zhu@erdw.ethz.ch (G. Zhu).

0031-9201/$ – see front matter. Crown Copyright © 2009 Published by Elsevier B.V. All rights reserved.
doi:10.1016/j.pepi.2009.10.008

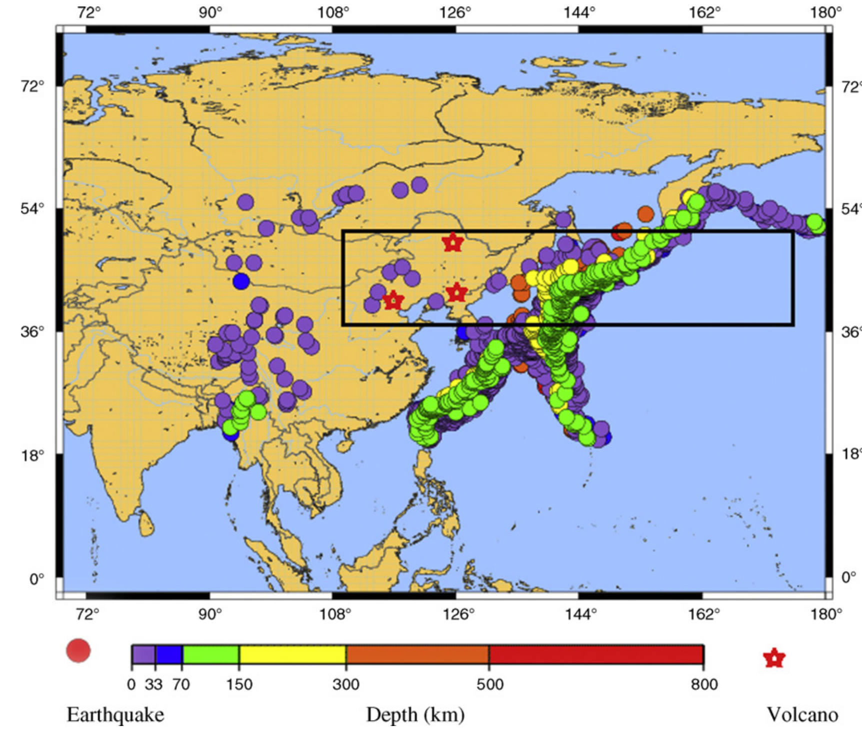

Fig. 1. The study area. Colored circles denote the earthquakes at different depths, red stars denote volcanoes in northeast China. The box with black solid lines denotes our model domain. The figure is produced from the official website: http://www.iris.edu. (For interpretation of the references to color in this figure legend, the reader is referred to the web version of the article.)

of volcanism in NE China (Liu and Wang, 1982; Liu et al., 2001) and relative Pacific Plate motion to Eurasian Plate during Cenozoic Times (Northrup et al., 1995). Our simulations are helpful to improve our understanding of its possible subduction process and its corresponding geophysical phenomena.

2. Constraining data

Plate motion can be decomposed into plate velocities from subduction and trench motion in a certain reference frame (Faccenna et al., 2007; Bellahsen et al., 2005). Trench migration is based on the

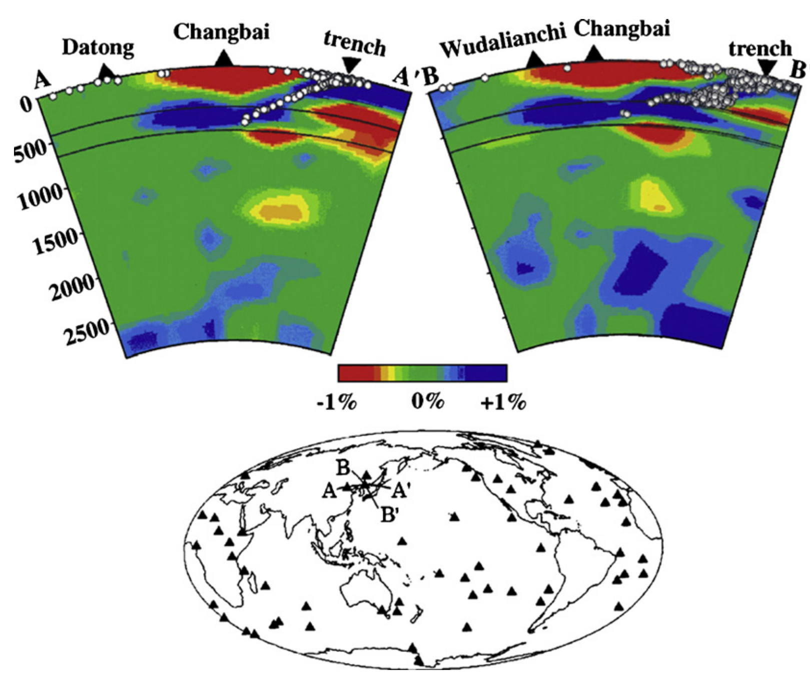

Fig. 2. Vertical cross-sections of P-wave velocity images determined by a global tomographic inversion (Zhao, 2004). Locations of the cross-sections are shown in the insert map. Red and blue colors denote slow and fast velocities, respectively. The velocity perturbation scale is shown below the cross-sections. Black triangles denote volcanoes. The reversed triangles show the location of the Japan Trench. White dots denote earthquakes that occurred within 150 km of the profiles. The two solid lines denote the 410 and 660 km discontinuities. Reproduced with permission. (For interpretation of the references to color in this figure legend, the reader is referred to the web version of the article.)

influence of mantle flows and related to many parameters, such as slab width (Schellart et al., 2007; Stegman et al., 2006), slab age (Heuret and Lallemand, 2005), and upper plate motion (Faccenna et al., 2007; Bellahsen et al., 2005). Back-arc extension/compression represents the trench motion with respect to upper plate motion. What we can directly observe is the back-arc extension on the surface. Following this idea, we hypothesize that the migration rate of magmatism towards the trench in the eastern margin of Asia can be regarded as the trench retreat rate and we also regard the motion of the Pacific plate relative to Eurasia plate as the relative motion of the oceanic lithosphere to local fixed Euro-Asian reference frame, that is, the left boundary of the model is the reference point, as shown in Fig. 1.

2.1. Migration of volcanic activity in NE China

The migration of magmatism eastwards in an extensional tectonic setting in late Mesozoic and Cenozoic times is a quite common feature along the eastern Asian continental margin, including the eastern coast of China, the Korean peninsula and southwest Japan (Kinoshita, 1995; Zhou and Li, 2000; Itoh and Tsuru, 2006), although there is strong magma mixing with a multi-episodic and multicycled process (Guo et al., 2007; Shi and Wang, 1993; Ma and Wu, 1987; Liu et al., 1995). This might be related to the distant effect of the Pacific plate subduction (Shi and Zhang, 2004). The Cenozoic volcanic rocks in eastern China are part of the Circum-Pacific volcanic belt that lies behind the Japanese-Izu-Bonin-Mariana-Philippine calc-alkalic volcanic arcs that festoon the western side of the Pacific Ocean (Zhou and Armstrong, 1982). However, there are some key questions about the time of subduction of the Pacific plate relative to the Eurasian plate and the trench retreat velocity. Liu (1987) has analyzed that the Cenozoic magmatic activity in NE China induced by subduction of the Pacific plate underneath the Asiatic continent started at the end of the Paleocene or in the early Eocene (56 Ma). Several aspects of trench retreat have been discussed in Shi and Zhang (2004), (40)–90 mm/year (Turcotte and Schuber, 2001) can also be obtained within possible cases. The age of volcanic rocks inferred from geochronological studies for northeast China shows that the velocity of the retreating trench is approximately 45 mm/year (Liu and Wang, 1982; Liu, 1989; Liu et al., 2001).

2.2. Relative motion of Pacific plate to Eurasian plate

There are many research studies on plate motion using geological data in different reference frames for plate reconstructions (Molar and Stock, 1987; Lithgow-Bertelloni and Richards, 1998; DeMets et al., 1990; Müller et al., 1993; O'Neill et al., 2003; Torsvik et al., 2008; Steinberger, 2008). However, few research studies have systematically studied the relative motion of Pacific plate to Eurasian plate in the Cenozoic period (Northrup et al., 1995), especially with geodynamical numerical methods (Liu et al., 2008).

Taking the Eurasian plate as a fixed reference frame, the convergence rate of the Pacific Plate to Eurasia Plate can be regarded as the Pacific Plate motion rate relative to the Eurasian Plate, which meets the needs of our research. Northrup et al. (1995) have made an analysis of the motion of the Pacific plate relative to the Eurasian Plate from the late Cretaceous period to present, assuming that the Pacific and Eurasian plates were in contact during the Cenozoic period. From a late Cretaceous convergence rate of 120–140 mm/year, the rate declined substantially during the early Tertiary period and reached a minimum of 30–49 mm/year in the Eocene period. In the Oligocene to earliest Miocene period, the average convergence rate increased moderately to 70–95 mm/year, then decreased again to 65–70 mm/year during the early to middle Miocene period. From the late Miocene to the present, the rate of convergence increased to an average of 100–110 mm/year. For details, see (Northrup et al., 1995, Fig. 2).

Table 1
Uniform physical and geometrical parameters of all models.

Parameter	Value
Temperature, T	
Pressure, P	
Velocity, u	
Thickness of fluid layer, D	1.90×10^6 m
Rayleigh number, Ra	4.07×10^7
Outer radius, R_0	6.37×10^6 m
Reference density, ρ_0	3.3×10^3 kg m^{-3}
Reference viscosity, η_0	1.0×10^{22} Pa s
Thermal conductivity, k	3.0 W m^{-1} K^{-1}
Thermal diffusivity, κ	10^{-6} m^{-2} s^{-1}
Acceleration of gravity, g	10 m s^{-2}
Thermal expansion, α	3.0×10^{-5} K^{-1}
Lithosphere (thickness; viscosity η; c1; c2)	(0–90 km; η_0; 1.9187; −1.177)
Asthenosphere (thickness; viscosity η; c1; c2)	(90–410 km; 0.02η_0; 1.9187; −1.177)
Transition zone (thickness; viscosity η; c1; c2)	(410–670 km; 0.4η_0; 2.0595; 0.75647)
Lower mantle (thickness; viscosity η; c1; c2)	(670–1900 km; 10η_0; 2.0595; 0.75647)

3. Methods and model description

The three-dimensional (3D) spherical software CitcomS (Zhong and Zuber, 2000; Tan et al., 2006), is used to model a spherical region with linear rheology. Fluid flow is assumed to be incompressible with infinite Prandtl number and the Boussinesq approximation is made, leading to the basic nondimensional equations (e.g., Turcotte and Schuber, 2001) as follows (Zhong and Zuber, 2000):

$$\mu_{i,j} = 0 \tag{1}$$

$$-p_i + (\eta u_{i,j} + \eta u_{i,j})_{,j} + \xi Ra T \delta_{ir} = 0 \tag{2}$$

$$T_{,t} + u_i T_i = T_{,ii} \tag{3}$$

where all symbols are defined in Table 1, Ra, the Rayleigh number, and ξ are defined as

$$Ra = \frac{\rho g \alpha \Delta T D^3}{\eta_0 \kappa}; \quad \xi = \frac{R_0^3}{D^3}$$

Eqs. (1)–(3) are nondimensionalized in the following way: $x_i = R_0 x_i'$, $u_i = (\kappa/R_0)u_i'$, $T = \Delta T T' + T_0$, $t = (R_0^2/\kappa)t'$, $\eta = \eta_0 \eta'$, $P = (\eta_0 \kappa / R_0^2)P'$. The primes are dropped in Eqs. (1)–(3).

The dynamic viscosity η is assumed to be temperature-dependent: $\eta = \eta_0 \exp((c_1/T + c_2) - (c_1/1 + c_2))$, where c_1 and c_2 are constants and η_0 is the viscosity at nondimensional temperature T = 1. For these simplified test models, we use Newtonian rheology.

Basing parameters on the observational data and geodynamical discussion with some uncertainties, we carried out a set of calculations to check the effect of the trench retreat velocity in our models. A 3D model is used because slab width will significantly affect slab retreat (Funiciello et al., 2003a,b; Stegman et al., 2006; Schellart et al., 2007). Our simulation domain is the longitude from 110° to 175°, and the latitude from 35° to 50°, as is shown in Fig. 1. Since we focus on the characteristics of the subducting slab above the 670 km discontinuity, four layers are included in radius: 0–90 km, 90–410 km, 410–670 km and 670–1910 km, corresponding to the lithosphere, asthenosphere, transition zone, and lower mantle. Physical and geometric parameters are given in Table 1. All calculations have an isothermal surface T = 0 and isothermal bottom T = 1 in the nondimensional Eq. (3), adiabatic sidewalls,

Table 2
Model descriptions.

Models	Age of subduction	Imposed trench retreat velocity	Convergence rate
1	70–50 Ma	0 km/Ma	106 km/Ma
	49–0 Ma	45 km/Ma	106 km/Ma
2	30–0 Ma (initialized subduction slab to transition zone)	11 km/Ma	106 km/Ma
3	50–0 Ma (without initialized subduction slab to transition zone)	11 km/Ma	106 km/Ma
4	70–50 Ma	0 km/Ma	106 km/Ma
	49–0 Ma	17 km/Ma	106 km/Ma
5	75–69 Ma	0 km/Ma	126 km/Ma
	58–53 Ma	0 km/Ma	75 km/Ma
	52–39 Ma	17 km/Ma	36 km/Ma
	38–29 Ma	22 km/Ma	76 km/Ma
	28–19 Ma	29 km/Ma	90 km/Ma
	18–10 Ma	44 km/Ma	61 km/Ma
	10–0 Ma	44 km/Ma	102 km/Ma

and Rayleigh number $Ra = 4.07 \times 10^7$. The mechanical boundaries are: imposed velocity at the surface and impermeable sidewalls and bottom boundary. All models with different surface velocities are described quantitatively in Table 2. The internal geodynamical processes evolved according to the above equations, and can be compared with tomographic results. The initial condition consists of a continental plate on the left side with an oceanic plate on the right side, with the subduction zone located at the distance of 20° from the left boundary. The nondimensional initial temperature gradients are, respectively, 1/13 for 225 km thick continental plate (left part) and 1/10 for 130 km thick for oceanic plate (right part), and the nondimensional initial interior temperature is set to 1.

4. Results

The results of our models can be compared with seismic tomography results (Huang and Zhao, 2006; Zhao et al., 2007). Here, we try to reproduce the geodynamical processes according to geological data, compare the final (present day) state with tomography results, then improve the models gradually, including the initial subduction time, trench retreat velocity and oceanic plate velocity, with details shown in Table 2.

The convergence rate between the Pacific Plate and the Eurasian Plate has been estimated systematically by Northrup et al. (1995). Our regional models adopt the Eurasian Plate as the local reference frame, that is, the left boundary of numerical simulation domain, as shown in Fig. 1. We regard convergence rate as oceanic plate velocity in our model, and the reference area is the stable area (110–124°), that is, the continental extension starts from 124° located in NE China. Therefore we suppose these convergence rates are quite certain in the Cenozoic period, and we firstly explore the proper trench retreat velocity. The following cases are designed to understand the effect of the trench retreat. Firstly, we investigate internal geodynamic processes with a higher present day convergence rate (Northrup et al., 1995) and trench retreat velocity (Liu, 1989; Liu et al., 2001) as the surface boundary condition. In model 1, we suppose that the trench did not retreat during 70–50 Ma, adopt a trench retreat velocity of 45 mm/year (Liu et al., 2001) during 50–0 Ma and take the convergence rate of 106 mm/year in the most recent 10 Ma as the constant subduction rate of the oceanic plate. Assuming that continental lithosphere converged towards the oceanic plate at a linearly increasing velocity with a small magnitude of less than 10 mm/year, which is relative to the left endpoint of the model during 70–29 Ma, the reference area is the stable area (110–124°) since 29 Ma. In order to be comparable with geological data, we focus on the results of thickness of lithosphere, velocity field and normalized temperature field in three scenarios (respectively in stages of 70–50 Ma, 50–29 Ma and 29–0 Ma). The time evolution of nondimensional temperature at 0.85 (Fig. 3a) indicates that subduction initiated at 70 Ma, and the slab arrived at the transition zone at 50 Ma. In the following 20 Ma, the subducting slab enters the transition zone. The subduction angle becomes smaller as the subduction zone retreats, and the tip of the slab gradually lies down in the transition zone. Velocities (Fig. 3b and d) indicate that during 70–50 Ma the subducting slab was pushing upper mantle material downwards, the upper mantle material was moving forward in the transition zone, and asthenospheric material underneath the continental lithosphere was moving towards the flow corner. A big convection cell formed between the oceanic plate and the 660 km discontinuity. During 50–29 Ma, the shallow slab could

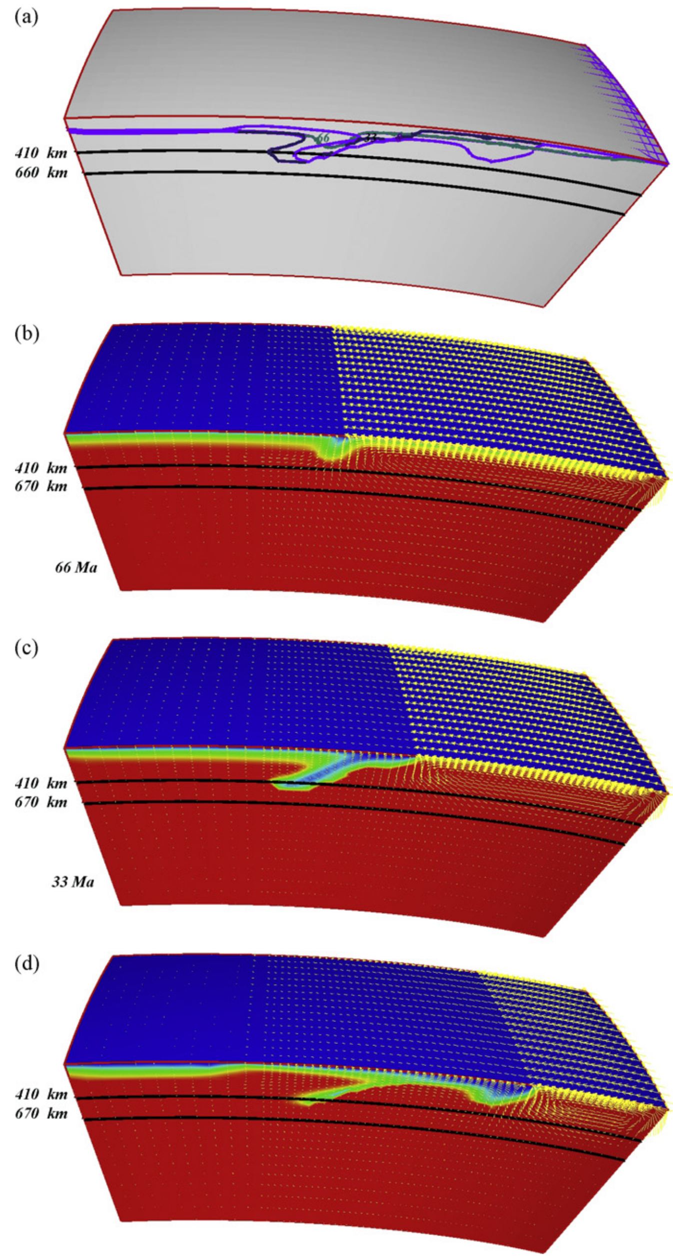

Fig. 3. Model 1: (a) nondimensional isotherms (0.85) at different times, which represent the evolution of the lithospheric thickness with time. (b–d) Velocities and normalized temperature fields with time, respectively. These show the shape of the slab during the subduction process, and can be compared with tomography.

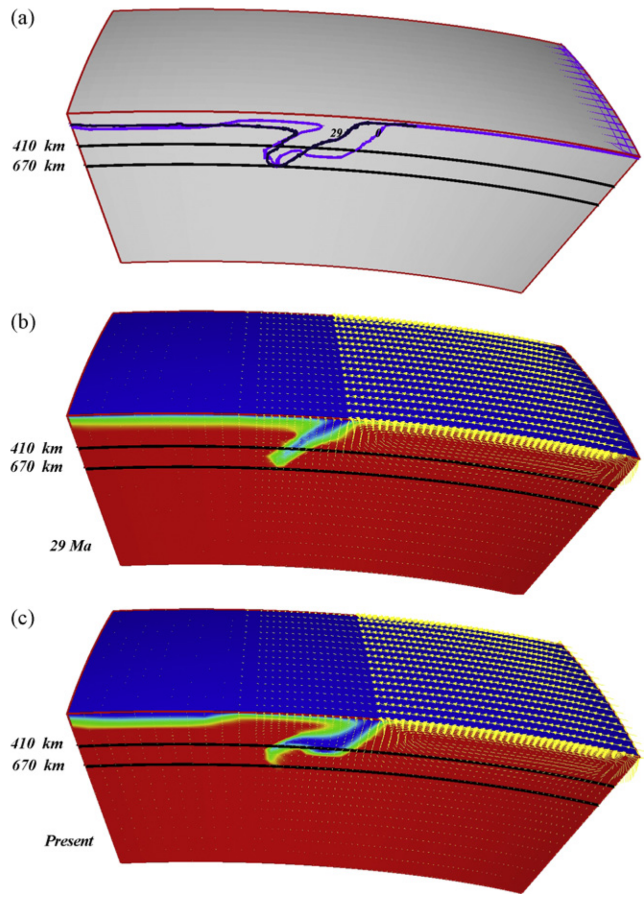

Fig. 4. Model 2: (a) nondimensional isotherms (0.85) with time showing back-arc extension and slab thickening in the transition zone. (b) and (c) Velocities and normalized temperature fields at 29 Ma B.P. and the present day, respectively. Velocities show material migration during the subduction process.

take all the asthenospheric material underneath the continental lithosphere towards the trench with the help of trench retreat. The tip and middle part of the slab displaced little. During 29–0 Ma, the trench continued retreating and the local area of continental lithosphere extended but the tip of the slab did not move forwards, instead lying down in the transition zone. The whole convection cell has cut the slab, which can possibly lead to the break-off of the slab (Gerya et al., 2004). The temperature field also shows that the slab does not have enough time to accumulate in the transition zone due to the high retreat velocity of the trench (Fig. 3b and d). In this model, the extension of Japan Sea during the last 50 Ma is too much. This is not consistent with geological observations, which show that back-arc extension of the Japan Sea started at about 28 Ma (Liu et al., 2001), with the Japan sea expanding about 400 km during 22–15 Ma and a total extension of nearly 900 km. The results of this case show that the retreat velocity of the trench should be less than 45 mm/year.

The next step (Model 2) is to test how long the slab can lie in the transition zone, with reduced the trench retreat velocity as 11 km per Ma, and an about 180 km thick initial subducting slab with dip angle 45° penetrating into the transition zone at 30 Ma, the initial temperature increases from $T = 0$ at the center of the slab to $T = 1$ at the slab-mantle interface. Seen from Fig. 4, a back-arc basin forms due to trench retreat, and grows with time. Slow trench retreat helps the slab to lie down or thicken in the transition zone. The lithosphere becomes thinner with time, with the thinnest part located at the edge of the stable continental lithosphere. In Fig. 4b and c, a small-scale convection cell appears above the slab, and involves more sub-continental material with increasing time. The trend of material migration is the same as in model 1. However, the length of the lying slab is about 400 km, which is much less than in the tomographic result. The dip angle of the slab is even bigger, which indicates that the trench should retreat faster or subduction should begin earlier. Models 1 and 2 have given us the estimate of the trench retreat velocity, that is, the range is between 45 km/Ma and 11 km/Ma.

Model 3, without an initial subducting slab, is to test how long it takes for the subducting slab to arrive in the transition zone with the assumed viscosity structure. Assuming that the slab subducted since 50 Ma, the continental lithosphere is assumed to extend linearly towards the trench with a small magnitude during 50–29 Ma, and to extend linearly towards stable area (110–124°) during 29–0 Ma. The imposed velocity on the oceanic plate is the same as that in model 2. As can be seen from the process of subduction (Fig. 5(a)), the subducting slab has arrived at the 410 km discontinuity by 29–28 Ma, but has not penetrated into the transition zone. The dip angle of the subducting slab becomes smaller with time, and the tip of the slab thickens and penetrates into the transition zone. In Fig. 5(b), one big convection cell has formed above the slab, and the tip of the subducting slab is advancing. The slab pushes material in the transitional zone upwards, supplementing the convection cell. After the slab has retreated, a small-scale convection cell forms and material from both the transition zone and the sub-continental asthenosphere join the small-scale convection cell, as can be seen in Fig. 5(c). However, the length of the lying slab is shorter than what is indicated by tomography (Huang

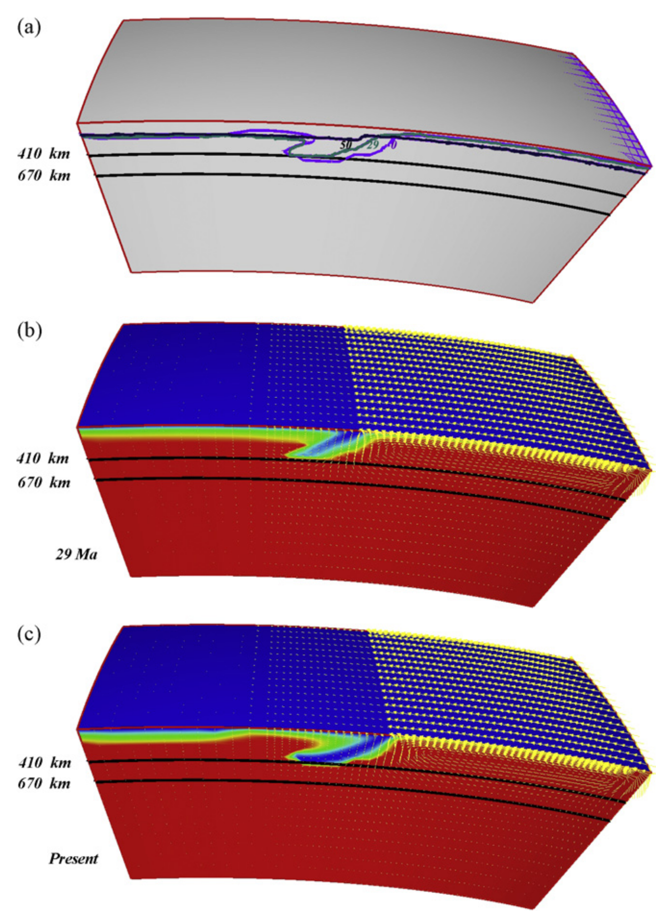

Fig. 5. Model 3: (a) nondimensional isotherms (0.85) with time showing back-arc extension and thickening of the slab in the transition zone. (b) and (c) Velocities and normalized temperature fields at 29 Ma B.P. and the present day, respectively. Velocities show material migration during the subduction process.

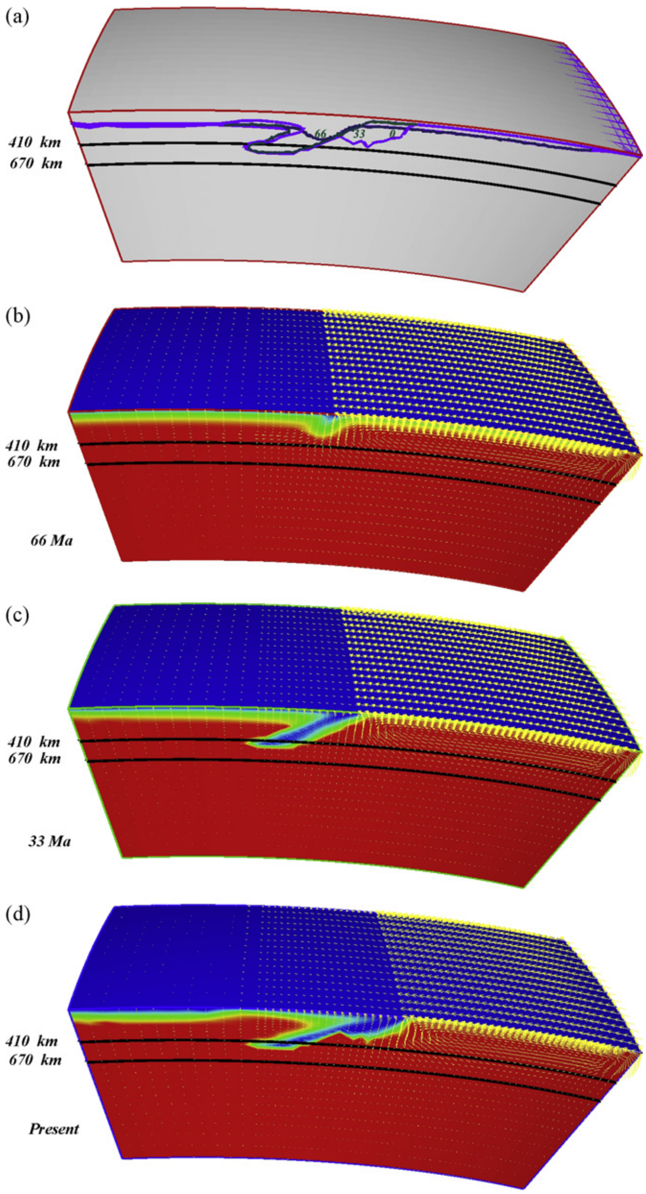

Fig. 6. Model 4: (a) nondimensional isotherms (0.85) with time (b–d) velocities and normalized temperature fields with time. Velocities show material migration during the subduction process.

and Zhao, 2006; Zhao et al., 2007), which might be because more time is needed for the slab to go into the transition zone, which in turn indicates that the initial subduction should occur earlier than 50 Ma.

It is clear that the slowness of the trench retreat and the longer initial subduction time affect the shape of the subducting slab. Now we improved our model (model 4) by lengthening the initial subduction time and adjusting the trench retreat velocity to 17 km per Ma. Seen from Fig. 6(a), the slab can lie down and become thickened in the transition zone after it has had enough time to penetrate into the transition zone. In Fig. 6(b) and (d), velocities show the process of the subduction, the early downwards motion of upper mantle material due to slab driving, and then slab penetration into the transition zone. However, the slab has no choice but to lie down in the transition zone because of the high viscosity lower mantle. Unlike the velocity field in model 1, the velocity vectors in the convection cell above the slab no longer cut across the slab (Fig. 3(c)), but rather, go along the subducting slab (Fig. 6(c)). But the length of the flat-lying slab is still shorter than what is indicated by tomographic images.

Up to now, we can estimate that the proper trench retreat velocity is less than 45 km/Ma (Liu, 1989; Liu et al., 2001), and that the initial subduction may occur earlier than 70 Ma. However, the detailed trench retreat velocity is still uncertain. In model 5, we impose a gradually increasing trench retreat velocity from 17 km/Ma to 44 km/Ma and convergence rate according to the paper by Northrup et al. (1995). In the whole subduction process (Fig. 7(a)), the slab dip angle became lower with time, the tip of the slab lays in the transition zone, and the slab dip angle becomes lower and lower in the shallow region. The shape of the subducting slab (blue in Fig. 7(d)) looks like the high velocity structures in the seismic tomography (Huang and Zhao, 2006; Zhao et al., 2007) (Fig. 1), and the flat-lying slab is about 600 km long. However, the extensional distance in this model is up to 1400 km, longer than the extension of Japan Sea, which is about 900 km. This discrepancy might be caused by neglecting uneven extension processes in the back-arc area.

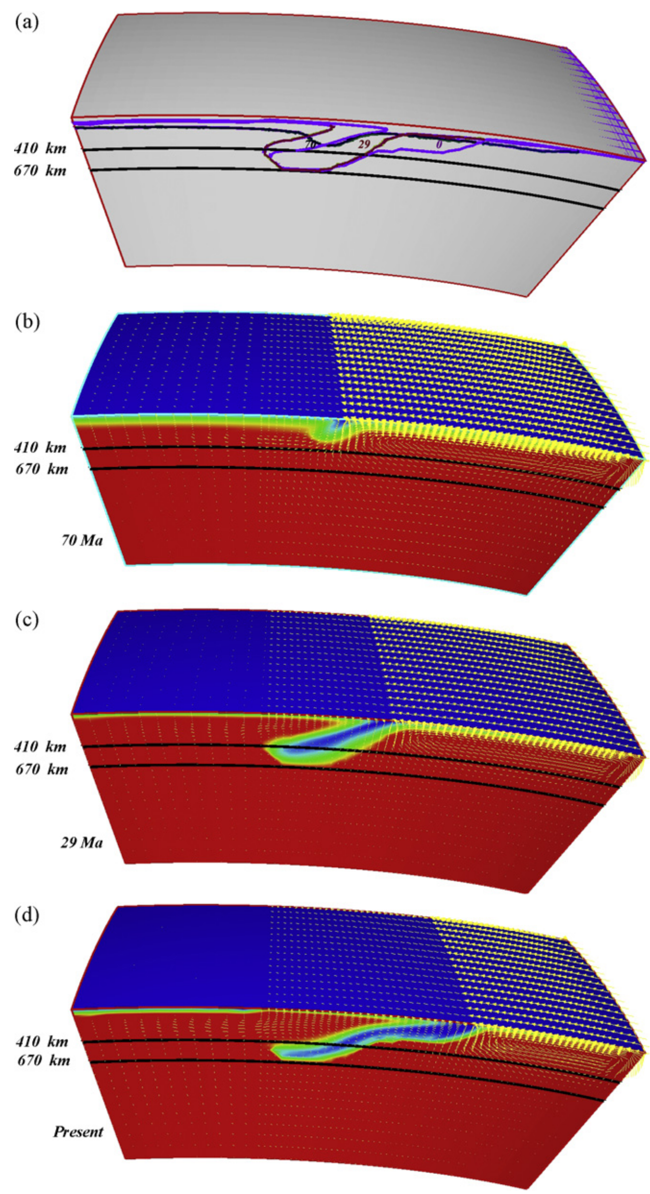

Fig. 7. Model 5: (a) nondimensional isotherms (0.85) with time (b–d) velocities and normalized temperature fields with time. Velocities show material migration during the subduction process.

The velocity field shows that mantle material underneath the continental lithosphere was pushed forward during the initial stage of subduction (see Fig. 7(b)), and the slab has to move forwards slowly or lie down in the transition zone due to the obstacle of the high viscosity lower mantle. Trench retreat helps to generate a small convection cell above the subducting slab, and material in the transition zone does not move forwards, but rather upwards to compensate for the convection cell (see Fig. 7(c)). The basin extended and continental lithosphere became thinner with the rapid retreat of the slab, while the shallower slab was moving towards the ocean (Fig. 7(d)), which provides the possibility of towards-ocean migration of the volcanoes in NE China.

5. Discussion

The results of our models with different patterns of imposed velocities at the surface help us understand the geodynamical process corresponding to the subduction of the Pacific Plate underneath Northeast China, assuming that a high viscosity contrast between the upper and lower mantle makes the slab lie flat in the transition zone instead of penetrating into the lower mantle. Several factors are also taken into account in our models. The first is the characteristics of trench retreat velocity, the second is the approximate initial time of the subduction, and the third one is material migration.

Different patterns of trench retreat velocity can significantly influence the shape of the subducting slab (Christensen, 2001; Guillou-Frottier et al., 1995). The faster the trench retreats, the flatter the slab is. With the constraints of tomographic results and geological analysis of convergence rates of Pacific-Eurasian plates, our model indicates that a trench retreat velocity of 44 km per Ma is too fast, but 11 km per Ma is too slow. If the trench retreats too fast, the slab can break-off due to the over extension; if it is too slow, the slab tends to sink down because of its negative buoyancy. From our models, we can estimate that the trench retreat velocity should less than 45 km/Ma, as is estimated by some geologists, but we cannot give an exact figure for it. However, one gradually increasing velocity pattern gives similar results to tomography results, but not precisely to reconstruct the subduction process.

The initial time of subduction is also tested by changing the starting time. If the subduction starts earlier, then there is enough time for the slab to penetrate into the transition zone and thicken. The results from our models show that the subduction of the Pacific Plate under the Eurasian Plate is most likely to have occurred since 70 Ma. In addition, the velocity fields in all models presented here have one common feature regarding the material migration during the subduction process. Mantle material underneath the continental lithosphere was pushed forward during the initial stage of subduction. After the slab arrived in the transition zone, the materials underneath Northeast China and in the transition zone move upwards to compensate the corner flow above the slab. It may indicate our expectation from the subduction process: with the current increasing trench retreat rate, the possible force for the trench retreat is the eastern oriented asthenospheric flow response to trench retreat and pushing effect underneath the continental lithosphere, which may be related to Indian-Eurasian collision (An et al., 1998; Liu et al., 2004). In order to realize this expectation in the future, we need develop a more self-consistent subduction model including a weak zone or fault in the subduction channel, to understand the kinematic and dynamical processes.

There is another shortcoming of our model. We always assume that continental crust is extended evenly, but the real case is much more complicated. Sometimes the Japan Sea extends, sometimes the continental lithosphere under Northeast China extends, and/or extension happens episodically. In model 5, the total extension is nearly 1400 km, but the actual extension of Japan Sea is almost 900 km, so the other 500 km extension is possibly distributed in Northeast China or North China. Hence, additional actual geological constraints should be studied.

Acknowledgements

Thanks for Dr. S. Zhong and Eh Tan to answer for the usage about the CitcomS2.2.2 software from CIG projects. Thanks for Dr. D. Zhao to explain for tomography results. TecPlot software is used in this paper. Special appreciation to the Editors of PEPI for encouragement. Supported by an SNF grant. SNF grants 200021-116381/1, 200020-126832/1, NSFC Grant 90814014.

References

An, M.J., Shi, Y.L., Li, F.Q., 1998. Genetic algorithm-finite element method inversion of the factors determining the recent tectonic stress field of part of East Asia area. Seismol. Soc. China 11 (3), 265–272 (in Chinese).

Becker, T.W., Faccenna, C., O'Connell, R.J., Giardini, D., 1999. The development of slabs in the upper mantle: insights from numerical and laboratory experiments. J. Geophys. Res. 104 (15), 207–215.

Bellahsen, N., Faccenna, C., Funiciello, F., 2005. Dynamics of subduction and plate motion in laboratory experiments: insights into the "plate tectonics" behavior of the Earth. J. Geophys. Res. 110, B01401, doi:10.1029/2004JB0029999.

Bi, S.W., 1997. Earth system science and sustainable development (II) the research on the dynamics model and plume tectonics features of the universal theory of the tectonics. Syst. Eng. Theory Pract. 7, 59–68 (in Chinese).

Christensen, U., 2001. Geodynamic models of deep subduction. Phys. Earth Planet. Int. 127, 25–34.

DeMets, C., Gordon, R.G., Argus, D.F., Stein, S., 1990. Current plate motions. Geophys. J. Int. 101, 425–478.

Duncan, R.A., Richards, M.A., 1991. Hotspots, mantle plumes, flood basalts, and true polar wander. Rev. Geophys. 29, 31–50.

Faccenna, C., Heuret, A., Funiciello, F., Lallemand, S., Becker, T.W., 2007. Predicting trench and plate motion from the dynamics of a strong slab. Earth Planet. Sci. Lett. 257, 29–36.

Funiciello, F., Faccenna, C., Giardini, D., Regenauer-Lieb, K., 2003a. Dynamics of retreating slabs: 2. Insights from three-dimensional laboratory experiments. J. Geophys. Res. 108 (B4), 2207, doi:10.1029/2001JB000896.

Funiciello, F., Morra, G., Regenauer-Lieb, K., Giardini, D., 2003b. Dynamics of retreating slabs: 1. Insights from two-dimensional numerical experiments. J. Geophys. Res. 108 (B4), 2206, doi:10.1029/2001JB000898.

Gerya, T.V., Yuen, D.A., Maresch, W.V., 2004. Thermomechanical modeling of slab detachment. Earth Planet. Sci. Lett. 226, 101–116.

Guillou-Frottier, L., Buttles, J., Olson, P.A., 1995. Laboratory experiments on the structure of subducted oceanic lithosphere. Earth Planet. Sci. Lett. 133, 19–34.

Guo, F., Nakamura, E., Fan, W.M., Kobayashi, K., Li, C.W., 2007. Generation of Palaeocene adakitic andesites by magma mixing; Yanji area. J. Petrol. 48 (4), 661–692.

Huang, H.L., Zhao, D.P., 2006. High-resolution mantle tomography of China and surrounding regions. J. Geophys. Res. 11, B09305, doi:10.1029/2005JB004066.

Heuret, A., Lallemand, S., 2005. Plate motions, slab dynamics and back-arc deformation. Phys. Earth Planet. Inter. 149 (1–2), 31–51.

Itoh, Y., Tsuru, T., 2006. A model of late Cenozoic transcurrent motion and deformation in the fore-arc lf northeast Japan: constraints from geophysical studies. Phys. Earth Planet. Inter. 156, 117–129.

Kinoshita, O., 1995. Migration of igneous activities related to ridge subduction in Southwest Japan and the East Asian continental margin from the Mesozoic to the Paleogene. Tectonophysics 245, 25–35.

Liu, G., 1987. The Cenozoic rift system of the North China plain and the deep internal process. Tectonophysics 133, 277–285.

Liu, J.Q., Han, J.T., Fyfe, W.S., 2001. Cenozoic episodic volcanism and continental rifting in northeast China and possible link to Japan Sea development as revealed from K–Ar geochronology. Tectonophysics 339 (3–4), 385–401.

Liu, J.Q., Wang, S.S., 1982. Formation times of Changbaishan volcano and Tianchi Lake. Chin. Sci. Bull. 21, 1312–1315 (in Chinese).

Liu, J.Q., 1989. On the origin and evolution of continental rift system in northeast China. Chin. J. Geol. 3, 209–216 (in Chinese).

Liu, M., Cui, X., Liu, F., 2004. Cenozoic rifting and volcanism in eastern China: A mantle dynamic link to the Indo-Asian collision? Tectonophysics 393, 29–42.

Liu, R., Xie, G., Zhou, X., Chen, W., Fan, Q., 1995. Tectonic environments of Cenozoic volcanic rocks in China and characteristics of the source regions in the mantle. Chin. J. Geochem. 14 (4), 289–302 (in Chinese).

Liu, L., Spasojević, S., Gurnis, M., 2008. Reconstructing Farallon Plate Subduction beneath North America back to the Late Cretaceous. Science 322, 934–938, doi:10.1126/science.1162921.

Lithgow-Bertelloni, C., Richards, M.A., 1998. The dynamics of cenozoic and mesozoic plate motions. Rev. Geophys. 36 (1), 27–78.

Ma, X., Wu, D., 1987. Cenozoic extensional tectonics in China. Tectonophysics 133, 243–255.

Molar, P., Stock, J., 1987. Relative motions of hotspots in the Pacific, Atlantic and Indian oceans since late Cretaceous time. Nature 327, 587–591.
Molnar, P., Tapponnier, P., 1975. Cenozoic tectonics of Asia: effects of a continental collision. Science 189, 419–426.
Molnar, P., Tapponnier, P., 1977. Relation of the tectonics of eastern China to the India-Eurasia collision: application of slip-line field theory to large-scale continental tectonics. Geology 5, 212–216.
Müller, R.D., Royer, J.Y., Lawver, L.A., 1993. Revised plate motions relative to the hotspots from combined Atlantic and Indian Ocean hotspot tracks. Geology 21, 275–278.
Northrup, C.J., Royden, L.H., Burchfiel, B.C., 1995. Motion of the Pacific plate relative to Eurasia and its potential relation to Cenozoic extension along the eastern margin of Eurasia. Geology 23 (8), 719–722.
O'Neill, C., Müller, R.D., Steinberger, B., 2003. Geodynamic implications of moving Indian Ocean hotspots. Earth Planet. Sci. Lett. 215, 151–168.
Schellart, W.P., Freeman, J., Stegman, D.R., Moresi, L., May, D., 2007. Evolution and diversity of subduction zones controlled by slab width. Nature 446, doi:10.1038/nature05615.
Shi, Y.L., Wang, Q.Y., 1993. The roll-back of subduction zone and the back-arc e × tension. Acta Geophys. Sinica 36 (1), 37–43 (in Chinese).
Shi, Y.L., Zhang, J., 2004. Deep geodynamics of far filed intercontinental back-arc extension formation of cenozoic volcanoes in northeastern China. Acta Seismol. Sinica 26 (Suppl.), 1–8 (in Chinese).
Stegman, D.R., Freeman, J., Schellart, W.P., Moresi, L., May, D., 2006. Influence of trench width on subduction hinge retreat rates in 3-D models of slab rollback. Geochem. Geophys. Geosyst. 7, Q03012, doi:10.1029/2005GC001056.
Steinberger, B., 2008. Reconstructing Earth history in three dimensions. Science 322, 866–868.
Sun, W.B., He, Y.S., 2004. The feature of seismicity in northeast China and its relation to the subduction of the Japan Sea plate. Seismol. Geol. 26 (1), 122–132.
Tan, E., Choi, E., Thoutireddy, P., Gurnis, M., Aivazis, M., 2006. GeoFramework: coupling multiple models of mantle convection within a computational framework. Geochem. Geophys. Geosyst. 7 (6), Q06001.
Turcotte, D.L., Schuber, G., 2001. Geodynamics, 2nd edition. Cambridge University Press, London.
Torsvik, T.H., Müller, R.D., Van der Voo, R., Steinberger, B., Gaina, C., 2008. Global plate motion frames: toward a unified model. Rev. Geophys. 46, RG3004, doi:10.1029/2007RG000227.
Zang, S.X., Ning, J.Y., 1996. Study on the subduction zone in western Pacific and its implication for the geodynamics. Chin. J. Geophys. 39 (2), 188–202 (in Chinese).
Zhao, D.P., 2004. Global tomographic images of mantle plumes and subducting slabs: insight into deep Earth dynamics. Phys. Earth Planet. Inter. 146, 3–34.
Zhao, D.P., Maruyama, S., Omori, S., 2007. Mantle dynamics of western Pacific to East Asia: new insight from seismic tomography and mineral physics. Gondwana Res. 11, 120–131.
Zhou, X.M., Li, W.X., 2000. Origin of Late Mesozoic igneous rocks in Southeastern China: implications for lithosphere subduction and underplating of mafic magmas. Tectonophysics 326, 269–287.
Zhou, X.H., Armstrong, R.L., 1982. Cenozoic volcanic rocks of eastern China—secular and geographic trends in chemistry and strontium isotopic composition. Earth Planet. Sci. Lett. 58, 301–329.
Zhong, S., Gurnis, M., 1997. Dynamic interaction between tectonic plates, subducting slabs, and the mantle. Earth Interact. 1 (3), 1–18.
Zhong, S., Zuber, M.T., 2000. Role of temperature-dependent viscosity and surface plates in spherical shell models of mantle convection. J. Geophys. Res. 105 (B5), 11063–11082.